Heterogeneous oxidation of nitrite anion by gas-phase ozone in an aqueous droplet levitated by laser tweezers (optical trap): Is there any evidence for enhanced surface reaction?

Oliver R. Hunt,[a,b] Andrew D. Ward,[b] and Martin D. King*[a]

Received Xth XXXXXXXXXX 20XX, Accepted Xth XXXXXXXXX 20XX
First published on the web Xth XXXXXXXXXX 200X
DOI: 10.1039/b000000x

The oxidation of nitrite anion within an aqueous atmospheric droplet may be a sink for HONO in the lower atmosphere. An optical trap with Raman spectroscopy is used to demonstrate that the oxidation of aqueous nitrite anion in levitated, micron sized, aqueous droplets by gas-phase ozone is consistent with bulk aqueous-phase kinetics and diffusion. There is no evidence of an enhanced or retarded reaction at the droplet surface at the concentrations used in the experiment or likely to be found in the atmosphere. The oxidation of nitrite in an aqueous droplet by gas-phase ozone does not cause the droplet to hygrodynamically change in size and demonstrates use of an optical trap as a wall-less reactor to measuring aqueous-phase rate coefficients.

1 Introduction

The photolysis of nitrate and nitrite in aqueous aerosol, rain, fog and snow is a source of atmospheric aqueous hydroxyl radical in atmospheric waters[e.g. [1–7]] and may be important in the oxidation of aqueous organic matter on atmospheric aerosol [e.g. [1]]. It has been suggested that there may be enhanced photolysis at the interface [8,9] owing to preferential solvation of nitrate anion at the air-water interface to the bulk. The surface of an aqueous solution of nitrite anion may be enhanced or depleted in nitrite anions, the evidence is not conclusive: Brown et al. [10] experimentally demonstrate that nitrite anion is depleted in the top 2-3nm of the 3M aqueous solution; whilst Otten et al. [11] experimentally demonstrate there is a strong surface adsorption of a sodium nitrite ion pair at the air-water interface of a molar solution of sodium nitrite. It is the aim of the work presented here to demonstrate that the propensity (or depletion) of nitrite anion at the air-water interface of a micron sized aqueous droplet does not effect its atmospherically important oxidation by gas-phase ozone and to *demonstrate that the oxidation by aqueous nitrite in micron sized droplets by gas-phase ozone is consistent with the liquid phase diffusion and reaction of ozone and no surface reaction is needed to explain the kinetics*.

The oxidation of nitrite anion by ozone,

$$NO^-_{2(aq)} + O_{3(aq)} \rightarrow NO^-_{3(aq)} + O_{2(aq)} \quad (1)$$

is important in the atmospheric chemistry of nitrite, e.g. [12], water treatment with ozone, e.g. [13–15] , and potentially in snow and ice photochemistry, e.g. [16,17]. The heterogeneous reaction was studied in a micron-sized aqueous droplet of sodium nitrite suspended in an optical trap in a gaseous background of humidified dilute ozone and air and studied by Raman spectroscopy. The optical trap allows the reaction to be studied in the spherical morphology found in the atmosphere, *i.e.* not touching any experimental support. [16,18–20] The volume of the droplet is controlled by the chemistry and size of the droplet and any large change in the size is atmospherically relevant and can be measured. The secondary aim of the work is to demonstrate that accurate measurement of aqueous-phase rate constants can be performed in tiny aqueous droplets held in an optical trap by laser Raman Tweezers. Such wall-less reaction vessels offer a unique experimental apparatus.

2 Experimental/Method

The trapping of the particle, reaction and particle production will be explained in three separate sections

2.1 Laser Tweezer Trapping

The laser tweezer, or optical, trap was formed by focussing a collimated 514.5 nm wavelength Ar-ion laser beam (Coherent Innova 90-5-UV) through a ×63, NA 1.2 water immersion objective mounted on a Leica DM-IRB microscope [19]. The laser power for trapping was ∼9 mW at the focal plane. Raman spectral signal from the droplet was collected, in a backscattering geometry, using the same objective lens as used

[a] *Department of Earth Sciences, Royal Holloway University of London, Egham, Surrey. Fax: 44 1784 471780; Tel: 44 1784 414038; E-mail: m.king@es.rhul.ac.uk*
[b] *Central Laser Facility, Research Complex at Harwell, Rutherford Appleton Laboratory, Harwell Innovation Campus, Chilton, Didcot, OX11 0FA, UK*

for optical trapping. After passing a notch filter the signal was directed through a spectrometer (Acton Research Corporation SP2500i, 1200 groove grating blazed at 500 nm) and recorded on a CCD (Princeton Instruments Spec10:400 BR/LN). The resolution on the detector was 1.006 rel cm^{-1} per pixel. Where rel cm^{-1} is the spectroscopic wavenumber from the Ar-ion laser at 514.5nm. Background Raman signal was acquired under identical conditions, but without a droplet, and was subtracted from the droplet spectra. The spectrograph was calibrated by comparison with the Raman spectra of toluene (Sigma-Aldrich, spectrophotometric grade). Raman spectra were taken of bulk solutions of sodium nitrite and sodium nitrate to determine the peak position due to each species. The nitrite peak occurred at $\sim$ 1049 rel cm^{-1}, which concurs with literature[21], and the nitrate peak occurred at $\sim$ 1333 rel cm^{-1}, which concurs with literature[22–26].

2.2 Experimental

The production of particles and gas-phase ozone is similar to our previous studies[27–29]. Briefly, the particles of aqueous nitrite were trapped in an aluminium trapping cell (volume $\sim$ 7cm^3) with two windows of borosilcate cover slips for entry and exit of the trapping laser. Gases and particles were fed into and out of the chamber via two $\frac{1}{4}$ inch tubes. The gas flow through the cell was a mixture of humidified nitrogen and dry oxygen at ambient pressure. The nitrogen gas-flow was humidified by bubbling through pure water at ambient temperature to produce a flow with a relative humidity of $> 95\%$ and assumed to be 100%. The combined flow of nitrogen and oxygen was 13.8 % v/v oxygen with a relative humidty of $\sim$ 86% and a total flow rate of 64.5$\pm$2.5 ml min^{-1} (the oxygen flow was 8.9 $\pm$ 0.2 ml min^{-1}) . Ozone was generated using a commercial ozoniser by photolysis of a flow of molecular oxygen with UV radiation from a mercury pen-ray lamp. The amount of ozone was controlled by shielding and un-shielding the lamp with an aluminium tube. The efficiency of the ozoniser and thus the concentration of ozone was calculated off-line by recording the UV-Vis spectra of the ozone produced and fitting to a known UV-Vis absorption cross-section[30]. Ozone mixing ratios of 6.8–30.9 ppm were used in the experiments described here. Repeat experiments were performed with the ozoniser switched off to ensure the decrease in nitrite anion concentration was due to reaction with ozone and not molecular oxygen. Analysis of the slow reaction between oxygen and nitrite anion allowed a rate constant to be estimated.

2.3 Particle production and reaction

Particles of aqueous sodium nitrite were produced by the ultrasonic nebulisation of solutions of 14.0 and 25.0 g L^{-1} (0.20 and 0.36 mol L^{-1}) sodium nitrite and blown gently into trapping chamber with air. The nebuliser was switched on and would remain on until a particle trapped in the laser focus and had grown to a size of $\sim$2-20 μm (but typically 7–12 μm for data presented here) by collisions with the trapped particle. The remaining particles in the cell were removed by air/nitrogen flow and collisions with the wall of the trapping cell within a minute.[19,20] The kinetic experiment begun almost immediately with Raman spectra co-added for 10 seconds and an optical image of the particle recorded every 60 seconds.

3 Kinetic Analysis

The rate of loss of nitrite anion (and the matching rate of production of nitrate anion) in an aqueous droplet depends on the concentration (and radial concentration profile) of ozone within the aqueous droplet. Thus the transport *and* reaction of ozone will be important i.e. gas-phase diffusion of ozone, surface accommodation, liquid-phase diffusion of the ozone. Section 3.1 highlights the important rate limiting processes and calculates the characteristic length scales for transport and reaction. Section 3.2 describes the application of analysis of Smith et al.[31] to determine a second order bimolecular rate equations for reaction 1 and section 3.3 corrects the rate constant determined in section 3.2 for ionic strength of the nitrite droplet.

3.1 Characteristic Times

Table 1 details the characteristic times for the different processes in the transport and reaction of ozone with a suspended droplet of aqueous nitrite solution[32]. Table 1 demonstrates the slowest process is the liquid-phase diffusion of ozone and that the diffuso-reactive length, l is an order of magnitude smaller than a typical radius of 5 μm.

3.2 Determination of the bimolecular rate coefficient

Smith et al.[31] demonstrated and described the mathematical framework for studying the uptake of gaseous species on liquid-phase reactants by considering the loss of the condensed phase species (nitrite anion in the example presented here). The significant advantage of their techniques is the non-reactive uptake of the gas-phase species is not confused with the reactive uptake. As shown in Table 1 the diffuso-reactive length, l, is less by a factor of 20 (closer to 40) than the particle's radius of 5 μm and the uptake coefficient can be calculated as the diffusion-limited special case[31] i.e. the ozone reacts close to the surface of the particle and rate of reaction proceeds at the rate of ozone diffusion into the droplet. Smith et al[31] derive the following relationship:

Table 1 The characteristic times for chemical reaction and transport in the oxidation of nitrite anion by gas-phase O_3. The following values have been used in this work: The diffusion constant for ozone in water, D_l, is estimated from the diffusion constant for oxygen in water as $2.1 \times 10^{-9} m^2 s^{-1}$,[33], with a mass accommodation coefficient, α, for ozone on an aqueous solution of 1×10^{-2},[30] the average molecular speed, $\bar{\nu}$ is 470 ms^{-1} the rate coefficient for reaction 1, k, is $3.7 \times 10^5 dm^3 mol^{-1} s^{-1}$,[34], a typical initial concentration of nitrite anion was taken as $0.36 mol\,dm^{-3}$, typical droplet radius is $5\,\mu m$, the diffusion coefficient of ozone in gas, D_l, is $1.76 \times 10^{-5} m^2 s^{-1}$,[33]. A Henry's law coefficient, H, for aqueous solution corrected for ion concentration and temperature is $10.32 mol\,m^{-3}\,atm^{-1}$, for a nitrite concentration of $0.36 mol\,dm^{-3}$ (and $11.04 mol\,m^{-3}\,atm^{-1}$ for a nitrite concentration of $0.20 mol\,dm^{-3}$)[30]. A gas constant, R, of $8.205 \times 10^{-5}\ m^3\,atm\,K^{-1}\,mol^{-1}$ for a temperature of 298 K is used.

Quantity	Estimate	Characteristic dimension
Diffuso-reactive length	$l = \sqrt{\frac{D_l}{k[NO_2^-]}}$	$0.12\,\mu m$
Gas-phase diffusion of ozone	$\frac{r^2}{\pi^2 D_g}$	144 ns
Accommodation	$D_l(\frac{4HRT}{\alpha\bar{\nu}})^2$	$\sim$ 100 ps
Liquid-phase diffusion of ozone	$\frac{r^2}{\pi^2 D_l}$	1.2 ms
Reaction	$\frac{1}{k[NO_2^-]}$	$7.3\,\mu s$

$$\sqrt{\frac{[NO_2^-]_t}{[NO_2^-]_{t=0}}} = 1 - \frac{3P(O_3)H\sqrt{D_l k}}{2r\sqrt{[NO_2^-]_{t=0}}}t \qquad (2)$$

where $[NO_2^-]_t$ is the concentration of nitrite anion at time, t in the aqueous droplet and $P(O_3)$ is the partial pressure of gas-phase ozone, all other variables defined in table 1. Thus for individual droplets by measuring $[NO_2^-]_t$ with time, t, and plotting $\sqrt{\frac{[NO_2^-]_t}{[NO_2^-]_{t=0}}}$ *versus* t, for individual particles will give a straight line with gradient $\frac{3P(O_3)H\sqrt{D_l k}}{2r\sqrt{[NO_2^-]_{t=0}}}$ and intercept 1. Plotting these gradients for individual particles versus $\frac{3P(O_3)H}{2r\sqrt{[NO_2^-]_{t=0}}}$ will yield a straight line with a gradient equal to $\sqrt{D_l k}$ i.e. giving the rate coefficient, k for reaction 1. A value of k similar to the literature value will confirm that the reaction can be explained by liquid phase kinetics and diffusion and no surface excess or depletion of nitrite needs to be invoked.

3.3 Correction for Ionic strength

The ionic strength of the nebulised droplet is large relative to the typical ionic strength measured in other studies determining the rate constants for reaction 1 as shown in table 3. Thus the rate coefficient determined by the analysis in section 3.2 should be corrected zero ionic strength for comparison with any literature value. Laidler[35] detail how the rate coefficient, k at ionic strength, I, can be related to the rate constant at zero ionic strength, k_0

$$\frac{k}{k_0} = e^{-b'I} \qquad (3)$$

where b' is treated as an empirical constant. A value of b' was estimated by fitting equation 3 to the data of Lagrange et al.[36] for the oxidation of sulphur by ozone in aqueous solution. A value of $b' = 1.25 \pm 0.031 dm^3 mol^{-1}$ was determined. Thus for an ionic strength of $\sim$0.36 mole dm^{-3} the rate constant would be a factor of 1.56 (1.55–1.58) larger than expected for an ionic strength of zero. The value of b' should be viewed as an estimate and the uncertainties in the values of b' much larger than the statistical values quoted.

3.4 Reaction with Oxygen

The presence of molecular oxygen in excess of ozone requires the study of the kinetics of the reaction of molecular oxygen with the aqueous nitrite anion to ensure the loss of nitrite anion is due to reaction with ozone and not molecular oxygen. Nitrite anion reacts slowly with molecular oxygen[37]. Experiments were performed with the ozoniser switched off to determine the effect of oxygen on nitrite anion oxidation and determined if the reaction of nitrite anion with oxygen influences the determination of the nitrite reaction with ozone.

4 Results

The results will be split into sections describing the results of the reaction of nitrite with ozone (section 4.1) and oxygen (section 4.2).

4.1 Reaction with ozone

Figure 1 demonstrates the loss of nitrite anion, and the consequent increase in nitrate anion in a 11.5 μm aqueous droplet. Figure 1 demonstrates that at the start of the reaction the droplet already contains some nitrate anion probably owing to either impurity in sodium nitrite salt or to the oxidation of the nitrite by oxygen present in the air during the ultrasonic nebulisation process that delivers aerosol to the trapping chamber. The data in figure 1 is replotted in figure 2 demonstrating the linear relationship expected from equation 2 and that the decay of nitrite anion concentration within the droplet is consistent with slow aqueous diffusion and relatively prompt reaction with ozone. Other processes limiting the kinetics such as surface-only reaction or loss of nitrite not limited by diffusion of ozone would display a exponential decay in figure 1[31]. In all, nine droplets were studied to completion, and plotted in a similar manner to figure 2 to determine the gradient as

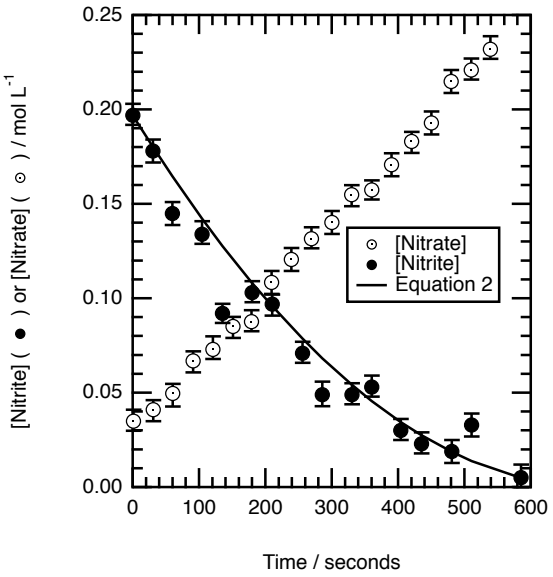

Fig. 1 The loss of nitrite(filled circles) and growth in nitrate (open circles) with time in a 11.5 μm droplets subjected to a $\sim$ 12 ppm atmosphere of ozone. The solid line is a fit of the concentration of nitrite anion to time using equation 2, *i.e.* $\sqrt{\frac{[NO_2^-]_t}{[NO_2^-]_{t=0}}} = 1 - Ct$, where C is determined empirically from the gradient of the graph (figure 2) and set equal to $\frac{3P(O_3)H\sqrt{D_l k}}{2r\sqrt{[NO_2^-]_{t=0}}}$.

shown in table 2. The gradient is equal to $\frac{3P(O_3)H\sqrt{D_l k}}{2r\sqrt{[NO_2^-]_{t=0}}}$ and plotting the gradient versus $\frac{3P(O_3)H}{2r\sqrt{[NO_2^-]_{t=0}}}$ will yield a straight line with a gradient equal to $\sqrt{D_l k}$. The gradient of figure 3 is equal to $\sqrt{D_l k}$ and $(1.0388\pm0.102)\times10^{-3}$ m$^{\frac{5}{2}}$ s mol$^{-\frac{1}{2}}$ (The uncertainty represents 1 standard deviation of the fit). Using a value of D_l of 2.1 $\times$ 10^{-9}m^{2}s^{-1},[33], gives a phenomenological rate constant k of 5.14$\pm$0.52 L mol^{-1} s^{-1}. The uncertainty is propagated uncertainty (two standard deviations) from the statistic uncertainty in fitting a straight line to the data in figure 3. Correcting the value of the rate constant for the effects of ionic strength of the solution according to section 3.3 gives a value of the second-order rate constant for reaction 1 of 3.29$\pm$0.32 L mol^{-1} s^{-1}. Comparison of the bimolecular rate constant determined in this work (k = 3.29$\pm$0.32 L mol^{-1} s^{-1}) with the literature values for same reaction in bulk solution are (contained in table 3) demonstrate excellent agreement suggesting that any surface enhancement of nitrate anion or depletion of nitrite anion at the droplet surface would have no measurable effect on the oxidation of nitrite anion in aqueous aerosol by gas-phase ozone.

The size of the droplet during reaction is plotted in Figure 4 during oxidation by either ozone (filled circles) or oxygen (open circles). Reaction 1 does change the hygrodynamic properties of the particles.

Table 3 Comparison of previous measurements of the rate constant for the aqueous reaction of nitrite anion by aqueous ozone, reaction (1).

Study	Ionic Strength / mol L^{-1}	Rate constants for reaction 1 k / L mol^{-1} s^{-1}
This Study	0.2 and 0.36	(3.3$\pm$0.32) $\times 10^5$
Damschen and Martin[38]	$(3-20)\times10^{-4}$	$(5.0\pm1.0)\times10^5$
Hoigne et al.[39]	$\sim 10^{-4}$	$(3.7\pm0.5)\times10^5$
Garland et al.[40]	$\sim 10^{-4}$	3.3×10^5
Penkett[41]	$\sim 10^{-4}$	$(1.60\pm0.13)\times10^5$
Liu et al[42]	~ 0.5	$(5.83\pm0.04)\times10^4$

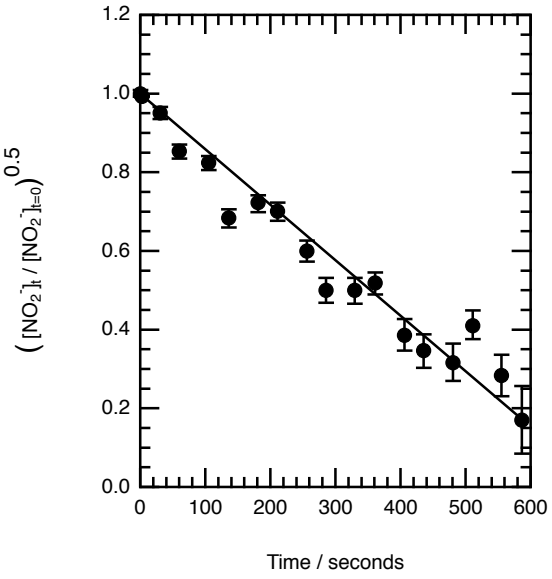

Fig. 2 The data in figure 1 presented as $\sqrt{\frac{[NO_2^-]_t}{[NO_2^-]_{t=0}}}$ *versus* reaction time, t. The linear relationship demonstrates a diffusion limited regime. The gradient of the linear regression is equal to $\frac{3P(O_3)H\sqrt{D_l k}}{2r\sqrt{[NO_2^-]_{t=0}}}$

4.2 Reaction with oxygen

The reaction between molecular oxygen and nitrite anion is slow and does not unduly effect the determination of the rate constant for reaction 1 between the nitrite anion and ozone. The diffusion of oxygen within the droplet is fast relative to reaction of nitrite anion with oxygen, i.e. the diffuso-reactive length is much greater than the particle radius. Thus the decay of nitrite and growth in nitrate can be seen at much slower rate in the absence of ozone and by the presence of oxygen within

Table 2 Experimental data from the nine droplets studied in detail reacting with ozone

$[NO_2^-]$ / mol L^{-1}	$P(O_3)$ / ppm	Droplet diameter / μm	Gradient $\frac{3P(O_3)H\sqrt{D_l k}}{2r\sqrt{[NO_2^-]_{t=0}}}$ / $10^{-3}s^{-1}$	Henry's Law coefficient / m^3 mol^{-1} atm^{-1}	$\frac{3P(O_3)H}{2r\sqrt{[NO_2^-]_{t=0}}}$ / $mol^{\frac{1}{2}}$ $m^{\frac{5}{2}}$
0.36	30.9	11.9	2.96	10.32	4.224
0.36	30.9	6.60	9.12	10.32	7.617
0.36	30.9	10.4	3.21	10.32	4.833
0.36	30.9	9.80	4.76	10.32	5.129
0.36	30.9	12.0	6.62	10.32	4.189
0.20	6.76	9.30	1.07	11.04	1.689
0.20	6.76	8.60	2.00	11.04	1.827
0.20	6.76	10.7	1.41	11.04	1.469
0.20	6.76	10.3	1.68	11.04	1.526

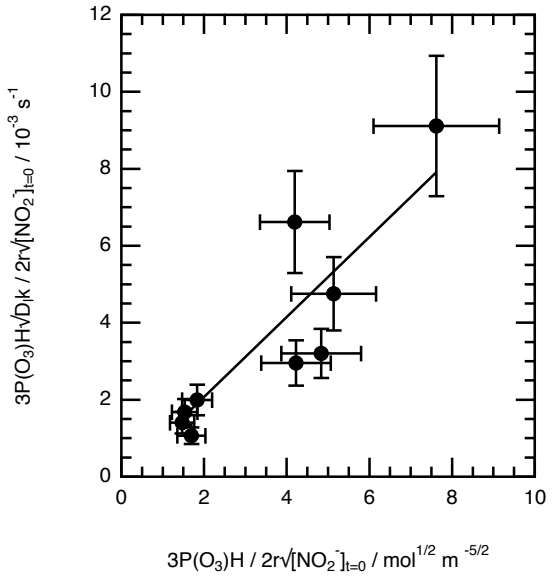

Fig. 3 The gradients of plots such as figure 2 and equal to $\frac{3P(O_3)H\sqrt{D_l k}}{2r\sqrt{[NO_2^-]_{t=0}}}$ are plotted against the calculated values of $\frac{3P(O_3)H}{2r\sqrt{[NO_2^-]_{t=0}}}$ (see table 3) and yield a straight line with a gradient equal to $\sqrt{D_l k}$. Errors bars are propagated uncertainty.

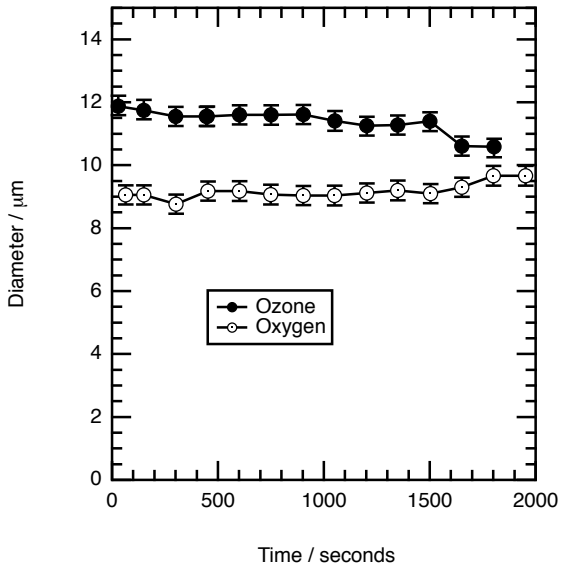

Fig. 4 Measured diameter of aqueous droplet of aqueous nitrite solution during oxidation by ozone (filled circles) and oxygen (open circles).

the air. Similar slower experiments to figure 1 were recorded and displayed in figure 5. The following kinetic equation[31], with diffusion fast relative to a slow liquid-phase reaction was fitted to the data in figure 5

$$\frac{[NO_2^-]_t}{[NO_2^-]_{t=0}} = e^{-P(O_2)Hkt} \quad (4)$$

A value of $P(O_2)Hk = (8.56 \pm 0.431) \times 10^{-4}$ s^{-1} was determined. The bimolecular rate constant between dissolved oxygen and nitrite is $\sim$5.2 L mol^{-1} s^{-1} using a value of H $\sim$1.2 mol m^{-3} atm^{-1} corrected for ion concentration and temperature[30].

5 Discussion

The discussion will focus on the experimental uncertainty, comparison to literature and the atmosphere implications.

5.1 Experimental uncertainty

The uncertainty reported on the rate coefficient for reaction 1 is a statistical uncertainty derived from the fitting of the exper-

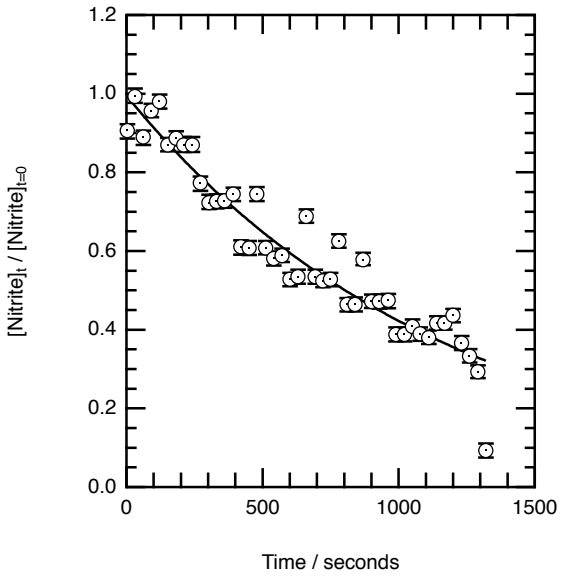

Fig. 5 The decay of nitrite anion within an aqueous droplet owing to reaction with molecular oxygen.The solid line is equation 4 fitted to the experimental points.

imental data in figure 2. The largest source of uncertainty in the derived rate coefficient is probably due to the value of b' as discussed in section 5.2 but even ignoring this correction for ionic strength would not change the conclusion of the study presented here. Further uncertainty in the concentrations of nitrite anion and ozone are not propagated into the uncertainty of the determination of the rate coefficient but are considered small compared with the reported statistic uncertainties.

5.2 Interpreting the results compared to literature

The rate coefficient for reaction 1 determined in this work is ($k = 3.3 \pm 0.32$ L mol^{-1} s^{-1}). Table 3 contains a comparison with the literature values measured in bulk and the agreement with previous literature studies is excellent. The concentration of nitrite anion used in the study is large compared to concentrations of nitrite anion measured in atmospheric cloud water and dew/fog (e.g. [12,43–45]) and thus the rate coefficient for reaction 1 has to be corrected by a factor of 1.56 (see section 3.3). The factor of 1.56 was estimated from a similar aqueous phase reaction of ozone, and may not be accurate. However values of b' calculated from the same study [36] for different ions suggest different, but similar values of b'. The previous determination of the rate constant for reaction 1 by Liu et al. [42] was performed at similar ionic strength to the study presented here and agrees well with the phenonomological rate constant reported in section 4.1. Ignoring the correction to the rate coefficient for reaction 1 would still provide agreement of the study presented here with at least one of the previous bulk studies [38] and not change the conclusion that any surface enhancement or depletion of nitrite at the droplet surface has any perceptible effect on the oxidation of nitrite in aqueous aerosol by gas-phase ozone.

5.3 Comment on the large concentrations used in this study

The concentrations used in this study may be large compared to atmospheric concentrations (see section 5.5) and such concentrations were necessitated by three issues: Raman spectroscopy not being a sensitive technique, the ability to record the kinetics in a reasonable length of time, and conducting the experiment with a small diffuso-reactive length. Ideally the diffuso-reactive length would have been smaller for the study described here i.e. a few nm instead of ~ 0.1 μm. The surface depletion or enhancement of nitrite anion is suggested to be important at a film depth of $\sim$ 3 nm. However this would require an increase in nitrite anion concentration of a factor of $\sim$1000 (see table 1) to achieve. The concentration of nitrite anion in these experiments is already a factor of 10^3 larger than that found in atmospheric hydrometers (see table 4). The results from this experiment show that the surface depletion or enhancement in the concentration of nitrite anion at the air-water interface is not important in the oxidation of nitrite by ozone at laboratory concentration and would therefore not be important at the lower concentrations found in the atmosphere. The agreement of the rate coefficient for reaction 1 as highlighted in section 5.2 with the literature values in table 5.2 does not suggest that the large concentrations of nitrite and ozone used in this study are detrimental to the aims of the study. It should be noted that in the atmosphere evaporating aerosol may form extremely concentrated solutions.

5.4 Comparison with the surface excess of aqueous nitrate solutions

Studies of the nitrate anion at the air-water interface [46–50] have shown an excess and a depletion of nitrate anion at the air water interface. However with the present state of knowledge the behaviour of the nitrate anion and nitrite anion at the air-water interface cannot be compared.

5.5 Atmospheric implications

Lammel and Cape [12] provide an overview of typical concentrations of nitrite anion found in atmosphere waters i.e. particles ($\sim 0.01 - 1$ ppbv), cloud water ($\sim 0.01 - 50\,\mu$mol dm^{-3}) and fog ($\sim 2 - 500\,\mu$mol dm^{-3}). with more recent measurements in the Amazon [51], Japan [52], Seoul [53], Chile [45], India [54], the Arctic [55], USA [56–58] and Europe [43,44,59–61]. Nitrite in atmospheric waters is important for (a) its involvement in the

multi-phase conversion of NO_x to Nitrous acid, HONO, which is an important source of atmospheric OH (e.g. [12,62–65]), (b) as a photolytic source of aqueous hydroxyl radical (e.g. [1–7]) and (c) its involvement in the nitration of phenols to produce air toxins [66,67]. An uptake coefficient for gas-phase ozone (owing to reaction with nitrite) on our experimental droplet may be estimated using equation 5 from [31]

$$\gamma = \frac{4HRT}{\bar{c}}\sqrt{Dk}\sqrt{\left[NO_2^-\right]} \quad (5)$$

to give a value of about 3×10^{-5}. Table 4 estimates the uptake of ozone on aqueous droplets due to reaction with nitrite anion for some common atmospheric particle containing atmospheric waters using equation 6 from [31]

$$\gamma = \frac{4HRT}{\bar{c}}\frac{r}{3}k\left[NO_2^-\right] \quad (6)$$

Pruppacher and Klett [68] suggest that particles that make up fogs have radii of 1.25 to tens of μm and a mean value of 5-10 μm, but inspection of their figure 2-4 on page 13 suggest the drop concentration distribution of fog droplets may be bimodal with typical radi around 1 and 15 μm. For clouds Pruppacher and Klett [68] note that the number distribution of cloud droplet diameters tends to become more smaller, more numerous and more homogenous in size in the order: orographic, stratus, marine cumulus and continental cumulus. Typical sizes for these cloud droplets have been taken from figure 2-11 in Pruppacher and Klett [68] .

The uptake coefficient is small but noticeably larger for fog particles. Rubio et al. [45] noted that the high concentration of nitrate anion found in fog particle relative to cloud may be a source of hydroxyl radical to the atmosphere.

6 Conclusions

The work presented here has demonstrated that any surface excess or depletion of nitrite anion at the air-water interface of an aqueous droplet does not effect the rate of oxidation of nitrite by gas-phase ozone. The work also demonstrates the use of laser Raman Tweezers and optical trapping for the simultaneous study of the particle morphology and kinetics for heterogenous reactions of atmospheric importance in a "wall-less" apparatus.

7 Acknowledgements

We gratefully acknowledge the support of the STFC (CM15C2/4 and CM11E2/05). The experiments were undertaken at the Central Laser Facility by all authors in 2005. ORH express gratitude to NERC (NE/H019103/1) and STFC for studentship support.

References

1 F. Karagulian, C. W. Dilbeck and B. J. Finlayson-Pitts, *J. Phys. Chem. A.*, 2009, **113**, 7205–7212.
2 D. Vione, V. Maurino, C. Minero, E. Pelizzetti, M. A. J. Harrison, R.-I. Olariu and C. Arsene, *Chem. Soc. Rev.*, 2006, **35**, 441–453.
3 J. L. France, M. D. King, J. Lee-Taylor, H. J. Beine, A. Ianniello, F. Domine and A. Macarthur, *J. Geophys. Res.-Atmos.*, 2011, **116**, F04013.
4 J. L. France, J. Lee-Taylor, H. J. Reay, M. D. King, D. Voisin, H.-W. Jacobi, F. Domine, H. J. Beine, C. Anastasio and A. Macarthur, *J. Geophys. Res.-Atmos.*, 2012, **117**, D00R12.
5 C. Anastasio and K. G. McGregor, *Atmos Environ*, 2001, **35**, 1079–1089.
6 T. Arakaki, T. Miyake, T. Hirakawa and H. Sakugawa, *Environ. Sci. Technol.*, 1999, **33**, 2561–2565.
7 M. Fischer and P. Warneck, *J. Phys. Chem. A.*, 1996, **100**, 18749–18756.
8 N. K. Richards, L. M. Wingen, K. M. Callahan, N. Nishino, M. T. Kleinman, D. J. Tobias and B. J. Finlayson-Pitts, *J. Phys. Chem. A. Phys Chem A*, 2011, **115**, 5810–5821.
9 L. M. Wingen, A. C. Moskun, S. N. Johnson, J. L. Thomas, M. Roeselová, D. J. Tobias, M. T. Kleinman and B. J. Finlayson-Pitts, *Phys. Chem. Chem. Phys*, 2008, **10**, 5668.
10 M. A. Brown, B. Winter, M. Faubel and J. C. Hemminger, *J. Am. Chem. Soc.*, 2009, **131**, 8354–8355.
11 D. E. Otten, R. Onorato, R. Michaels, J. Goodknight and R. J. Saykally, *Chem. Phys. Lett.*, 2012, **519-520**, 45–48.
12 G. Lammel and J. N. Cape, *Chem. Soc. Rev.*, 1996, **25**, 361–369.
13 W. Baozhen, T. Jinzhi, Y. Jun and S. Guangmei, *Ozone: Sci. Eng.*, 1989, **11**, 227–244.
14 S. Naumov, G. Mark, A. Jarocki and C. von Sonntag, *Ozone: Sci. Eng.*, 2010, **32**, 430–434.
15 C. Gottschalk and J. A. Libra, *Ozonation of Water and Waste Water: A Practical Guide to Understanding Ozone and its Applications*, Wiley-VCH, 2nd edn, 2009.
16 H.-W. Jacobi, J. Kleffmann, G. Villena, P. Wiesen, M. King, J. France, C. Anastasio and R. Staebler, *Environ. Sci. Technol.*, 2014, **48**, 165–172.
17 J. L. France, H. J. Reay, M. D. King, D. Voisin, H. W. Jacobi, F. Domine, H. Beine, C. Anastasio, A. MacArthur and J. Lee-Taylor, *J. Geophys. Res.-Atmos.*, 2012, **117**, year.
18 S. H. Jones, M. D. King and A. D. Ward, *Phys. Chem. Chem. Phys.*, 2013, **15**, 20735–20741.
19 O. R. Hunt, A. D. Ward and M. D. King, *RSC Adv.*, 2013, **3**, 19448–19454.
20 A. D. Ward, M. Zhang and O. Hunt, *Opt. Express*, 2008, **16**, 16390–16403.
21 J. T. Kloprogge, D. Wharton, L. Hickey and R. L. Frost, *Am. Min.*, 2002, **87**, 623–629.
22 H. Meresman, A. J. Hudson and J. P. Reid, *Analyst*, 2011, **136**, 3487–3495.
23 R. Symes, R. J. J. Gilham, R. M. Sayer and J. P. Reid, *Phys. Chem. Chem. Phys.*, 2005, **7**, 1414–1422.
24 M. H. Brooker and D. E. Irish, *Can. J. Chem*, 1970, **48**, 1198–.
25 K. Fung, D. Imre and I. Tang, *J. Aero. Sci.*, 1994, **25**, 479 – 485.
26 I. Tang and K. Fung, *J. Aero. Sci.*, 1989, **20**, 609 – 617.
27 M. D. King, K. C. Thompson, A. D. Ward, C. Pfrang and B. R. Hughes, *Faraday Discuss.*, 2007, **137**, 173–192.
28 M. D. King, K. C. Thompson and A. D. Ward, *J. Am. Chem. Soc.*, 2004, **126**, 16710–16711.
29 M. D. King, A. R. Rennie, K. C. Thompson, F. N. Fisher, C. C. Dong, R. K. Thomas, C. Pfrang and A. V. Hughes, *Phys. Chem. Chem. Phys*, 2009, **11**, 7699–7707.
30 S. Sander, R. Friedl, D. Golden, M. Kurylo, P. Wine, J. Abbatt,

Table 4 Estimated uptake coefficient for ozone on cloud and fog particles owing to reaction with nitrite. Uptake coefficients calculated with equation 6 using a value of $H \sim 10\text{mol m}^{-3}\text{atm}^{-1}$, R, of $8.205 \times 10^{-5}\ \text{m}^3\,\text{atm}\,\text{K}^{-1}\,\text{mol}^{-1}$, a temperature of 298 K, a molecular speed $\bar{c} = 353\ \text{m s}^{-1}$ a rate coefficient of k=$3.29 \times 10^2\ \text{m}^3\text{mol}^{-1}s^{-1}$ and values of r and $\left[NO_2^-\right]$ are contained within the table [12]

Cloud type	Typical radius (range) [68] / μm	Typical $\left[NO_2^-\right]$ (range) [12] / $\mu\text{mol dm}^{-3}$	Diffuso-reactive length , l / μm	Uptake Coefficient, γ / 10^{-10}
Fog	7.5 (1-30)	20 (2-700)	17.9	430
Fog	1 (1-30)	20 (2-700)	17.9	58
Fog	15 (1-30)	20 (2-700)	17.9	870
Orographic	20 (2.5-40)	0.1 (0.01-1)	252	6
Stratus	15 (2.5-30)	10 (1-20)	25.3	430
Marine Stratocumulus	13 (2-20)	1 (0.01-50)	252	38
Continental Stratocumulus	6 (2.5-10)	1 (0.01-50)	252	17

J. Burkholder, C. Kolb and G. Moortgat, *Chemical kinetics and photochemical data for use in Atmospheric Studies Evaluation Number 17*, Jet Propulsion Laboratory California Institute of Technology Pasadena, California Technical Report 17, 2011.

31 G. D. Smith, E. W. III, C. DeForest, T. Baer and R. E. Miller, *J. Phys. Chem. A.*, 2002, **106**, 8085–8095.

32 B. J. Finlayson-Pitts and J. N. J. Pitts, *Chemistry of the Upper and Lower Atmosphere: Theory, Experiments and Applications*, Acdemic Press, 2000.

33 E. L. Cussler, *Diffusion mass tranfer in fluid systems*, Cambridge University Press, 1999.

34 J. Hoigne, H. Bader, W. R. Haag and J. Staehelin, *Water Res*, 1985, **19**, 993–1004.

35 K. J. Laidler, *Chemical Kinetics*, Harper Collins Inc., 1987.

36 Lagrange, *J. Geophys. Res.-Atmos.*, 1994, **99**, 14595–14600.

37 P. K. Mudgal, S. P. Bansal and K. S. Gupta, *Atmos Environ*, 2007, **41**, 4097–4105.

38 D. E. Damschen and L. R. Martin, *Atmos. Environ. A.*, 1983, **17**, 2005–2011.

39 H. Hoigne and H. Bader, *Water Res*, 1983, **17**, 185–194.

40 J. A. Garland, A. W. Elzerman and S. A. Penkett, *J. Geophys. Res.-Atmos.*, 1980, **85**, 7488.

41 S. A. Penkett, *Nature*, 1972, **240**, 105–106.

42 Q. Liu, L. M. Schurter, C. E. Muller, S. Aloisio, J. S. Francisco and D. W. Margerum, *Inorg Chem*, 2001, **40**, 4436–4442.

43 K. Acker, D. Möller, R. Auel, W. Wieprecht and D. Kalaß, *Atmos Res*, 2005, **74**, 507–524.

44 K. Acker, D. Beysens and D. Moeller, *Atmos. Res.*, 2008, **87**, 200–212.

45 M. A. Rubio, E. Lissi and G. Villena, *Atmos. Environ.*, 2008, **42**, 7651–7656.

46 C. Tian, S. J. Byrnes, H.-L. Han and Y. R. Shen, *J. Phys. Chem. Lett.*, 2011, **2**, 1946–1949.

47 D. J. Tobias, A. C. Stern, M. D. Baer, Y. Levin and C. J. Mundy, *Ann. Rev. Phys. Chem.*, 2013, **64**, 339–359.

48 L. X. Dang, T. M. Chang, M. Roeselova, B. C. Garrett and D. J. Tobias, *J. Chem. Phys.*, 2006, **124**, 66101.

49 P. Salvador, J. E. Curtis, D. J. Tobias and P. Jungwirth, *Phys. Chem. Chem. Phys*, 2003, **5**, 3752.

50 J. L. Thomas, M. Roeselová, L. X. Dang and D. J. Tobias, *J. Phys. Chem. A.*, 2007, **111**, 3091–3098.

51 K. A. Mace, P. Artaxo and R. A. Duce, *J. Geophys. Res.-Atmos.*, 2003, **108**, year.

52 M. Takeuchi, H. Okochi and M. Igawa, *Bull. Chem. Soc. Japan*, 2002, **75**, 757–764.

53 C. H. Song, M. E. Park, E. J. Lee, J. H. Lee, B. K. Lee, D. S. Lee, J. Kim, J. S. Han, K. J. Moon and Y. Kondo, *Atmos. Environ.*, 2009, **43**, 2168–2173.

54 S. N. Sinha, N. M. Desai, G. M. Patel, M. M. Mansuri and V. Shivgotra, *J. Environ. Bio.*, 2010, **31**, 375–378.

55 S. M. Li, *Atmos Environ A-Gen*, 1993, **27**, 2959–2967.

56 K. F. Moore, D. E. Sherman, J. E. Reilly, M. P. Hannigan, T. Lee and J. L. Collett, *Atmos Environ*, 2004, **38**, 1403–1415.

57 S. Raja, R. Ravikrishna, R. R. Kommalapati and K. T. Valsaraj, *Environ. Mon. Ass.*, 2005, **110**, 99–120.

58 Q. Zhang and C. Anastasio, *Environ Sci Technol*, 2003, **37**, 3522–3530.

59 K. Acker, G. Spindler and E. Bruggemann, *Atmos. Environ. Environ.*, 2004, **38**, 6497–6505.

60 D. Beddows, R. J. Donovan, R. M. Harrison, M. R. Heal, R. P. Kinnersley, M. D. King, D. H. Nicholson and K. C. Thompson, *J. Environ. Monitor.*, 2004, **6**, 124–133.

61 K. A. Mace, N. Kubilay and R. A. Duce, *J. Geophys. Res.-Atmos.*, 2003, **108**, year.

62 B. J. Finlayson-Pitts, L. M. Wingen, A. L. Sumner, D. Syomin and K. A. Ramazan, *Phys. Chem. Chem. Phys*, 2002, **5**, 223–242.

63 T. Kinugawa, S. Enami, A. Yabushita, M. Kawasaki, M. R. Hoffmann and A. J. Colussi, *Phys. Chem. Chem. Phys*, 2011, **13**, 5144.

64 L. Wu, S. Tong and M. Ge, *J. Phys. Chem. A.*, 2013, **117**, 4937–4944.

65 S. M. Li, *J. Geophys. Res.-Atmos.*, 1994, **99**, 25469–25478.

66 M. Harrison, S. Barra, D. Borghesi, D. Vione, C. Arsene and R. Olariu, *Atmos. Environ.*, 2005, **39**, 231–248.

67 P. Patnaik and J. N. Khoury, *Water Res*, 2004, **38**, 206–210.

68 H. R. Pruppacher and J. D. Klett, *Microphysics of clouds and precipitation*, Kluwer Academic Publishers, Dordrecht/Boston/London, 2nd edn, 2003, vol. 18.

69 L. J. Moore, M. D. Summers and G. A. D. Ritchie, *Phys. Chem. Chem. Phys.*, 2013, **15**, 13489–13498.

70 L. Rkiouak, M. J. Tang, J. C. J. Camp, J. McGregor, I. M. Watson, R. A. Cox, M. Kalberer, A. D. Ward and F. D. Pope, *Phys. Chem. Chem. Phys.*, 2014, **16**, 11426–11434.